Spring 5-2017

Characterization of P43LGRN-3

Kelly G. Hill
University of Southern Mississippi

The University of Southern Mississippi

Characterization of P43LGRN-3

by

Kelly Hill

A Thesis
Submitted to the Honors College of
The University of Southern Mississippi
in Partial Fulfillment
of the Requirements for the Degree of
Bachelor of Science in the
Department of Chemistry and Biochemistry

May 2017

Approved by

_____

Vijay Rangachari, Ph.D., Thesis Adviser

Associate Professor of Biophysical Chemistry

_____

Sabine Heinhorst, Ph.D., Chair

Department of Chemistry and Biochemistry

_____

Ellen Weinauer, Ph.D., Dean

Honors College

Abstract

Alzheimer's Disease (AD) is a progressive neurodegenerative disorder characterized by extensive memory loss and cognitive deficits, which occur due to severe neuronal loss. Two hallmark lesions, intracellular neurofibrillary tangles composed of hyperphosphorylated tau and extracellular neuritic plaques formed by the aggregation of amyloid-β (Aβ), are responsible for the progressive neuronal loss seen in AD brains. Neurotoxic Aβ aggregates are also known to cause inflammation within the brain. It has recently come to light that severe and acute inflammation, such as seen in traumatic brain injury (TBI), may also lead to AD-type dementia. This has raised the question whether some of the pro-inflammatory mediators released from activated microglial cells could play a role in promoting the aggregation of Aβ and subsequent plaque formation. We hypothesize that a small family of cysteine rich, pro-inflammatory proteins called Granulins (Grns), which have been implicated in both AD and frontotemporal dementia (FTD), modulate Aβ aggregation. Based on the data obtained in our lab on GRN-3 protein, we have focused on P43LGRN-3, a missense mutant of GRN-3, which has been implicated in pathology. P43LGRN-3 was recombinantly expressed in *E. coli*, purified, and characterized by biochemical and biophysical tools. The effect of P43LGRN-3 on the binding and aggregation of Aβ was investigated via co-incubation experiments. The collected data suggest that monomeric P43LGRN-3 is largely similar to wild type GRN-3 (wt-GRN3) both structurally and functionally, and suggests the possible differences between the mutant and the wild-type protein could be more prominent with the precursor protein, progranulin. These data are presented and discussed.

Dedication

To all the grandparents I have lost,
I wish you were here to see this, but I know how proud you all are.

To my mom and dad,
Thank you for all of your unwavering support and love. I would not be the person I am today if it were not for you two. You are my dearest friends and biggest cheerleaders. I love you both so much.

Acknowledgements

I would like to thank my thesis advisor and mentor, Dr. Vijay Rangachari, for investing so much of his time into my education. You have taught me to be confident in myself in every situation and to never doubt my intelligence. I would also like to thank my graduate student, Gaurav Ghag. Out of everyone, I think you have taught me the most. You have been the greatest friend and role model. I thank you both for everything you have done for me.

Lastly, I would like to thank my Southern Miss family for the greatest four years of my life. I attribute my success to the innumerous faculty and staff members who identified my potential and encouraged me to challenge myself.

Thank you, Southern Miss, for leaving me better than you found me. I am forever grateful.

Table of Contents

Table of Contents

List of Figures

Chapter 1 - Introduction

Alzheimer's disease (AD) is an irreversible and progressive disease characterized by behavioral changes, memory loss, impaired judgment, and loss of cognitive function in patients above 60 years of age (1). AD is the most common among many neurodegenerative disorders that lead to dementia, being responsible for approximately 60-80% of the cases. The National Institute on Aging estimates that nearly 5.2 million Americans suffer from the disease, making AD the sixth leading cause of death in the United States. As life expectancy continues to increase, a dramatic escalation in the prevalence of AD is also expected, as there will be more individuals living past 65 years of age (2).

The aforementioned pathological traits of AD are caused by the progressive loss of neurons seen in AD brains. Two hallmark lesions cause this acute neuronal death, namely intracellular neurofibrillary tangles composed of hyper-phosphorylated tau protein and extracellular neuritic plaques, which are deposited on the brain due to the aggregation of a polypeptide called amyloid-β (Aβ). The aggregates of Aβ are known to trigger neurotoxicity. Aβ aggregates are also known to cause inflammation in the brain, whose mechanism has been widely investigated.

Increasing evidence in recent years has indicated that acute inflammatory reactions themselves may play a part in inducing the aggregation of Aβ, thereby triggering a vicious cycle of inflammation and aggregation. Evidence for this comes primarily from clinical studies on patients suffering from traumatic brain injury, who show AD symptoms sometimes within hours of sustaining the injury (5). In this context, pro-inflammatory mediators released by activated microglial cells may play an important

role (3). One such pro-inflammatory mediator that is released is a family of small, cysteine rich proteins called Granulins (GRNs). Granulins are cleaved from a larger precursor molecule that is anti-inflammatory in nature, called Progranulin (PGRN). The Progranulin protein is composed of 7.5 tandem repeats of different Granulin proteins (1-7) and Paragranulin (4). Granulin 3 (GRN-3) in particular has been shown experimentally to be pro-inflammatory in nature and has been previously characterized in the Rangachari lab. To further investigate the properties and potential role of Granulins in AD, a mutant form of GRN-3, P43LGRN-3, was chosen as this missense mutation has been implicated in frontotemporal dementia (FTD). Furthermore, based on the analyses by structural modeling, the P43L mutation is predicted to be pathogenic due to the destabilizing effect on protein structure and therefore function (30).

This honors thesis work involves the recombinant expression and characterization of P43LGRN-3 in *E. coli*, and the investigation of its further effect on Aβ aggregation.

Chapter 2 – Background

2.1 Amyloid-β and AD

AD is a debilitating neurodegenerative disease that results in declining cognitive function, loss of social appropriateness, and memory impairments. Based on genetic studies, animal modeling, and various biochemical data, it has been suggested that the aggregation of amyloid-β is responsible for the etiology of AD (6). As mentioned above, the senile or neuritic plaques characteristic of AD are primarily composed of extracellular deposits of Aβ peptides, which are formed via the proteolysis of a ubiquitous precursor protein called β-amyloid precursor protein (APP) (7,8). It has been observed that mutations in APP or presenilin genes that lead to overexpression of Aβ are seen in many familial forms of AD (9,10). Furthermore, individuals with Down syndrome who possess three copies of chromosome 21 – the chromosome housing the APP gene - develop pathologic symptoms of early-onset AD (10).

The monomeric protein has a high propensity for aggregation into oligomers and fibrils, which are known to be neurotoxic (11). However, it has been observed that cognitive decline occurs prior to the accumulation of plaques in transgenic mouse models, suggesting that low molecular weight soluble oligomers are the primary neurotoxic agents in AD pathology (12). Aβ aggregates are also known to induce inflammatory responses in which activated microglial cells release various cytokines, chemokines, along with other toxic species leading to neuronal death (13,14). The exact mechanism responsible for microglial activation and the subsequent release of neurotoxic pro-inflammatory mediators is unknown.

Conversely, there is evidence that suggests neuroinflammation as the primary cause for the onset of AD and of Aβ aggregation. Clinical studies have revealed increased levels of inflammatory proteins such as IL-6 present in the brain and plasma prior to the onset of dementia, suggesting that central nervous system (CNS) inflammation may be involved in the pathogenesis of AD (23). Furthermore, several more studies have shown the efficacy of prolonged use of non-steroidal anti-inflammatory drugs (NSAIDS) at reducing the risk of AD (24). It is believed that a subset of these drugs is responsible for selectively inhibiting the production of $A\beta_{42}$ peptides, the isomeric form of Aβ with the highest propensity to form aggregates (25,26). In this context, some external event such as a physical head injury/TBI or a severe infection acts as a stimulus for the initiation of the inflammatory cascade. In fact, a pathological link between TBI and AD onset is suspected based on the finding that up to 30% of patients who die following TBI have extracellular Aβ plaques strikingly similar to those seen in AD (27). These TBI-associated plaques can develop within hours after sustaining the injury, leaving the brain in a chronic state of inflammation thereby advancing the onset and progression of sporadic AD (5). The mechanism by which pro-inflammatory mediators released by the inflammatory cascade trigger initial Aβ aggregation remains unknown. This work is focused on reducing this knowledge gap by investigating whether there are direct interactions between Aβ and P43LGRN-3, which may potentially result in GRNs being established as key players in the molecular link between acute inflammation and AD.

2.2 Granulins and Neuroinflammation

As mentioned previously, Granulins are small, approximately 6 kDa, proteins that possess a motif of 12 cysteines consisting of four central pairs flanked by a single pair on the N- and C- termini (15). GRNs are released following the proteolytic cleavage of a precursor protein called progranulin (PGRN) by proteases like neutrophil elastase at linker regions between the GRN domains (4) (Figure 1). Human PGRN consists of seven and a half tandem repeats of Granulin domains (GRNs 1-7, and Paragranulin) and is known to have several biological functions including growth factor like activities, modulation of immune responses, wound repair, and neuronal effects. PGRN is overexpressed in tumors, including carcinomas, gliomas, and sarcomas (16,17,18), and is also believed to modulate cell proliferation pathways in tumor and neuronal cells (19,20).

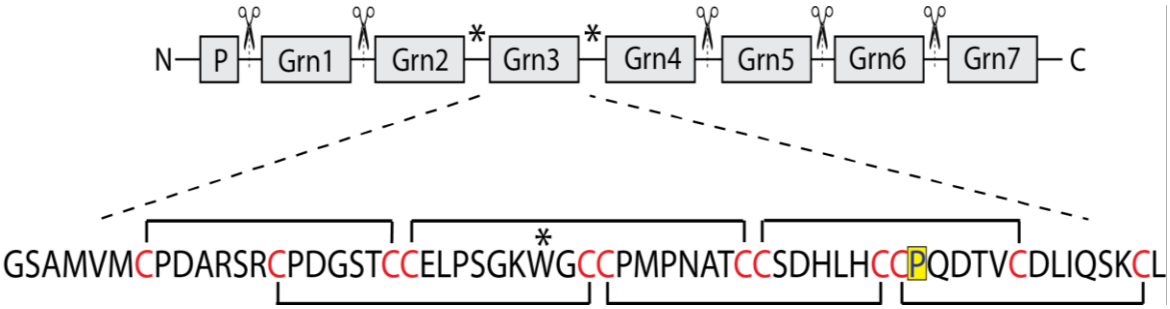

Figure 1: The Domain Structure of PGRN. The boxes indicate the individual GRN domains (1-7) with the amino acid sequence and putative disulfide-bonding pattern of GRN-3 below. The scissors denote the elastase cleavage sites. The asterisks denote linker regions where proteolytic cleavage occurs. The highlighted box around the Proline residue in the amino acid sequence indicates the position of the P43LGRN-3 mutation.

PGRNs and GRNs also play a role in neurodegeneration. It is known that mutations in the PGRN gene, located on chromosome 17, have been implicated in frontotemporal lobar dementia (FTLD) (21). FTLD is a neurodegenerative disorder characterized by behavior modification and altered personality; it is the second most

common presenile form of dementia after AD (22). More importantly, expression of PGRN as well as of the proteases that cleave it is elevated in microglial cells surrounding the senile plaques in AD patients. Consequently, the pro-inflammatory GRNs (1-7) that are secreted from microglial cells during inflammation are up-regulated in cases of TBI. Interestingly, PGRN inhibits the spreading of pro-inflammatory cytokines, while the individual GRNs stimulate the secretion of interleukin-8, thereby initiating an immune response. In other words, the full length PGRN protein has been implicated to be anti-inflammatory, while the GRNs are thought to be pro-inflammatory in nature (19,7). We hypothesize that acute inflammation triggered by other factors, such as TBI, activate microglial cells responsible for the cleavage of PGRN into the pro-inflammatory GRNs (4). Once secreted, these GRNs could interact with extracellular Aβ potentially augmenting its aggregation and therefore, modulating the onset of AD.

2.3 Why P43LGRN-3?

The physiological roles of individual GRN peptides are largely unknown at present and no concerted effort has been made to determine the activity of all seven. However, various partial characterizations have yielded information regarding a few. GRN-6 was found to be mitogenic for glioma cell lines and GRN-4 showed both mitogenic and growth inhibitory activities (17, 4). More promising, GRN-3 is suspected to stimulate interleukin-8 secretions thereby exerting pro-inflammatory effects in vivo (4). Furthermore, due to the incidence of PGRN mutations seen in FTLD patients, several mutations have been investigated. The majority of PGRN mutations are nonsense mutations resulting in mRNA decay and therefore decreased levels of PGRN protein, but

there are some missense mutations that occur within the signal sequence and the mature PGRN peptide (29). Two such missense mutations, p.Pro248Leu and p.Arg432Cys, have been found to drastically decrease the secretion of PGRN despite being actively expressed, with the P248L mutation reducing secretion up to 70%. The implications of decreased secretion of PGRN are unknown but it has been suggested that restoration of peptide levels to normal in cases with the above mentioned mutations may be a sufficient method for delaying onset or progression of AD (29). The p.Pro248Leu and p.Arg432Cys missense mutations have also been predicted to be pathogenic based on structural modeling. The Pro248Leu mutation, also referred to as P43LGRN-3, is suspected to have a significant destabilizing effect on the GRN-3 domain, thereby drastically affecting protein function (30). This conclusion is based on the probability of structure disruption based on location of the mutation within a loop connecting two β-hairpins (30).

2.4 Hypothesis and Research Objectives

We hypothesize that the P43L mutation located in the GRN-3 sequence will lead to structural changes within the protein as compared to the wild-type GRN-3. This purpose will be investigated through the scope of the following objectives:

1) Expression of P43LGRN-3 in *E. coli* cells
2) Purification using affinity chromatography and high performance liquid chromatography (HPLC)
3) Characterization of the biophysical properties
4) Investigating the effect of P43LGRN-3 on amyloid-β aggregation and binding
5) Comparison of P43LGRN-3 characteristics to that of wild-type GRN-3

Chapter 3 – Materials and Methods

3.1 Cloning and Expression of Human P43LGRN-3 in E. coli.

The P43LGRN-3 cDNA was commercially synthesized (Genewiz Inc.) and cloned into pET32b plasmid using NcoI and XhoI restriction sites. The cloning was carried out at the molecular cloning facility at the Florida State University. The pET32b enables expression of P43LGRN-3 as a thioredoxin fusion protein, P43LGRN-3-trxA. Thioredoxin facilitates disulfide bond formation in GRN-3 as the latter has six disulfide bonds. The pET32b:P43LGRN-3 plasmid was transformed and expressed using *E. coli* SHuffle competent cells (NEB). These cells have two distinct advantages: a) they carry mutations that maintain oxidizing conditions in the cytoplasm, which facilitate disulfide bond formation and, b) the cells express cytoplasmic disulfide bond isomerase (DsbC) that further enhances correct disulfide pairing. The cells containing the plasmids, pET32b:P43LGRN-3 were grown in a 2L baffled culture flasks containing one liter of LB broth medium supplemented with 100 μg mL^{-1} of ampicillin. The cells were grown till the optical density, measured using a UV-vis spectrophotometer at 600 nm, was between 0.5 – 0.6 AU. Isopropyl β-D-1-thiogalactopyranoside (IPTG) was then added to a final concentration of 0.1 mM to induce expression of the P43LGRN-3-trxA fusion protein. The IPTG was added when the optical density of the cells was between 0.5 and 0.7. The cells were harvested after six hours of growth at 30 °C with constant agitation at 250 rpm by centrifuging at 14000xg at 4°C for 10 minutes and were used immediately or stored at -20°C for later use.

3.2 Purification of Recombinant P43LGRN-3-trxA

Cell pellets collected from the 2 L culture were thawed at room temperature and then resuspended in a total of 30-40 mL of equilibration buffer (50mM Tris, 300 mM NaCl, 10mM imidazole, pH 6.5). The slightly acidic pH was maintained to minimize potential disulfide bond scrambling. Once resuspended in the buffer, 0.5 mM phenylmethylsulfonyl fluoride (PMSF) was added to prevent any proteolytic digestion. The cell suspension was then sonicated for a total of two minutes with 40 seconds bursts on ice and one minute rest. The suspension was then centrifuged at 9200xg to remove all cell debris. The supernatant from this step was loaded onto a Ni^{2+}-NTA column that was pre-equilibrated with the equilibration buffer. The supernatant was rocked with the beads for one hour at 4^{o}C to ensure maximum binding between nickel beads and the supernatant. After an hour, the supernatant was loaded onto the column and the flow-through was collected by gravity elution. The beads were then washed with 200 mL of wash buffer (50 mM Tris, pH 6.5, 300 mM NaCl, and 120 mM imidazole) to remove non-specific binding, and eluted using 50 mL of 400 mM imidazole in 50 mM Tris, pH 6.5, and 300 mM NaCl. In order to remove the imidazole, the protein was then dialyzed using a 10 kDa molecular weight cut-off (MWCO) semi-permeable membrane (Spectrum labs) at room temperature against a buffer with 2 mM Tris-HCl, pH 6.5, and 5 mM NaCl. The dialysate was then concentrated using a vacufuge such that the final buffer concentration was 20 mM Tris, pH 6.2 and 50 mM NaCl. After this, UV-Vis spectroscopy was used to measure the concentration of the fusion protein using a molar extinction coefficient of 20355 $M^{-1}cm^{-1}$ at 280 nm. The concentrated protein was aliquoted in 1 mL fractions and immediately incubated with restriction grade thrombin

(Novagen) (1U per 2 mg of protein) to cleave P43LGRN-3 from the P43LGRN-3-trxA fusion protein. The sample was incubated at 37 °C for 22-24 hours. The P43LGRN-3 protein was then fractioned using a semi-preparative Jupiter® 5 μm C18 reverse phase HPLC column (Phenomenex, CA) with height and internal diameter of 250 mm and 10 mm, respectively, and a gradient of 80 – 60 % acetonitrile containing 0.1% TFA.

3.3 SDS-PAGE, MALDI-ToF and Free Thiol Quantification

The purity of the protein was assessed using SDS-polyacrylamide gel electrophoresis (PAGE) and MALDI-ToF mass spectrometry (Bruker Daltonics Inc). SDS- PAGE was performed using 8-16% Mini-Protean precast gels (BioRad). The protein samples were subjected to reducing or non-reducing 4X Laemmli buffer with and without boiling. Gels were stained using a Pierce silver staining kit (Thermo Scientific) and imaged using a GelDoc molecular imager (BioRad).

For MALDI-ToF, one microliter of sinnapinic acid (SA) matrix was mixed with one microliter of protein sample on a MSP 96 microchip target (Bruker) to yield a final protein concentration of 0.01-0.1 nM. The SA matrix was made by resuspending 10 mg of SA in one milliliter of 1:1 acetonitrile:water with 0.1%TFA.

To check the integrity of disulfide bonds, the sample was analyzed by SDS-PAGE under reducing and non-reducing conditions. Since GRN-3 contains six disulfide bonds, the integrity of the disulfide bonds was analyzed using Ellman's assay. This assay uses Ellman's reagent [2,2'-dithiobis-(2-nitrobenzoate)] which reacts with free sulfhydryls (thiols) to form a yellow colored product whose intensity can be estimated by measuring UV-absorbance at 412 nm and used to calculate the percentage of free cysteines.

Alkylation experiments were also performed on the samples in which 2-4 μg of P43LGRN-3 was incubated with 2000x molar excess of iodoacetamide solution in presence of 1000x molar excess of guanidium hydrochloride at room temperature for 90 min to overnight in the dark. Alkylation of the protein was analyzed using MALDI-ToF.

3.4 Fluorescence Spectroscopy

A Cary Eclipse spectrometer (Agilent Inc.) was used to perform fluorescence measurements. The samples were excited at 280 nm to measure the fluorescent emissions from intrinsic tryptophan residues within the protein sequence. The excitation and emission slits were set at 10 or 20 nm. Binding interactions between P43LGRN-3 and Aβ peptides was assessed using intrinsic fluorescence assay as well. Aβ peptides were titrated onto P43LGRN-3 and changes in emission spectrum for each titration were monitored. The sample was excited at 290 nm to avoid excitation of tyrosine residues, which excite at ~276 nm. The fluorescence was monitored at 350 nm with a bandwidth of 10 nm.

3.5 Circular Dichroism (CD)

To assess the secondary structure, the protein was analyzed using a Jasco J-815 CD spectrometer. Using a 1 mm path length quartz cuvette (Helma), the samples were monitored under continuous scanning mode from 260 to 198 nm with a scanning speed of 50 nm/min. The data integration time was set at 8 seconds, bandwidth at 1 nm, and data pitch at 0.1 nm. Each Far-UV CD spectra obtained was representative of an average of three scans.

3.6 Interactions of P43LGRN-3 and Aβ

Effects of P43LGRN-3 on Aβ aggregation were analyzed by co-incubating P43LGRN-3 with Aβ at varying stoichiometric concentrations, and monitoring aggregation by Thioflavin T (ThT) fluorescence assay, immunoblotting, and circular dichroism. For the ThT assay, the samples were diluted 15-fold using 10 μM ThT prepared in 20 mM Tris-HCl, pH 8.0 or 6.5. Fluorescence measurements were taken for 1 minute with excitation and emission wavelengths at 450 and 482 nm, respectively. These co-incubated samples were also analyzed using SDS-PAGE and immunoblotting in parallel. For immunoblotting, the co-incubated proteins were transferred from the SDS gel to 0.45 μm pore size BioTrace^{TM} NT nitrocellulose membrane (PALL Life Sciences/BioRad) and blocked with 5% non-fat dry milk in 1x standard phosphate buffered saline (PBS), pH 7.4, with 0.1% Tween 20®. The blots were probed overnight with an Aβ42 specific antibody and then incubated with a Horse Radish Peroxidase (HRP)-conjugated secondary antibody for 1-2 hours. The blots were developed with enhanced chemiluminescence (ECL) substrate for 2 minutes (Thermo Scientific) and imaged using a GelDoc molecular imager (BioRad).

Chapter 4 - Results

4.1 Recombinant Expression of P43LGRN-3

4.1.1 Transformation and Purification

The pET32b:P43LGRN-3 plasmid was transformed into SHuffle competent *E. coli* cells using the heat shock method. The protein was expressed on a small scale (7 mL culture). Both induced and un-induced cultures were electrophoresed under reducing conditions on a 4-20% SDS-PAGE gel. An intense band, which is more prominent in the induced than the un-induced samples, is present at approximately 20 kDa as indicated by the arrow. (*Figure* 2). This corresponds to the 20.3 kDa molecular weight of P43LGRN-3-trxA protein. The protein expression was later scaled up to 1L cultures and purified as described in the Materials and Methods section.

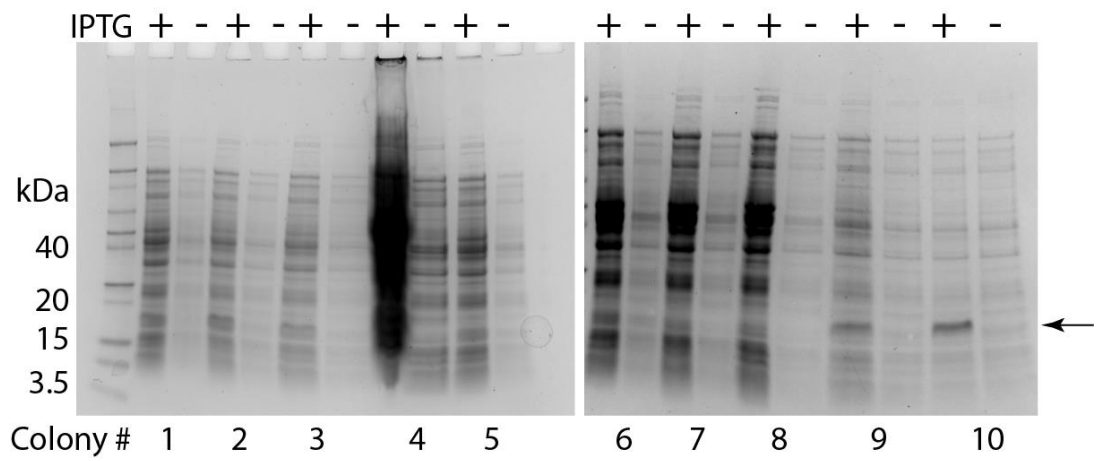

Figure 2: Small scale expression of P43LGRN-3-trxA in SHuffle *E. coli* cells containing the pET32b:P43LGRN-3 plasmid, analyzed on 4-20% SDS-PAGE gel. Both induced (+) and un-induced (U) colonies exhibit band under 20 kDa (highlighted with arrow). Band is darker in induced lanes.

To confirm the presence of the P43LGRN-3-trxA protein, aliquots from each step of the purification (pellet, supernatant, flow-through, wash 1, wash 2, and strip) were taken and subjected to electrophoresis on a 4- 20% SDS-PAGE gel (*Figure 3).* An intense band seen in the elution fraction at approximately 6 kDa confirmed the presence of the target protein. The eluate was then dialyzed and the concentration was calculated using a UV-Vis spectrometer. Prior to HPLC, thrombin digestion was performed to separate the P43LGRN-3 protein from its thioredoxin fusion.

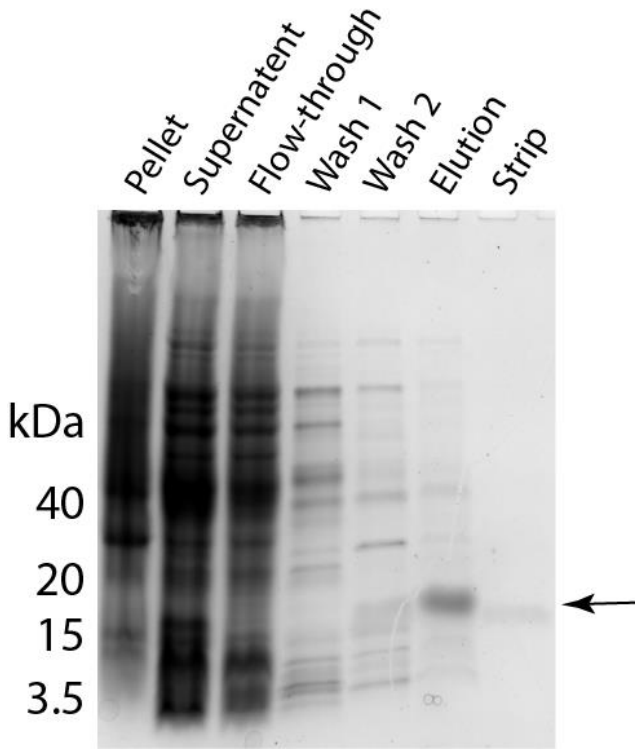

Figure 3: Ni-NTA Purification of thioredoxin fusion protein. In the elution lane, a dark band, highlighted by the arrow, indicates the presence of P43LGRN-3-trxA.

4.1.2 HPLC Analysis

P43LGRN-3 monomer was isolated using a reverse phase C-18 HPLC column with a gradient of 80-60% acetonitrile with 0.1 % TFA. The resulting HPLC profile for P43LGRN-3 can be seen in Figure 4A. Peaks have been labeled with their corresponding fraction number. Fraction 46 is suspected to be the monomeric fraction as indicated by the (M) above the peak. Figure 4B shows the HPLC profile of the wild-type GRN-3

protein, in which Fraction 48 corresponds to monomeric GRN-3. It is noteworthy that the fractionation profile of P43LGRN-3 indicated that the mutant is able to generate a significantly lesser degree of multimeric GRN-3 as compared to the wild-type protein (Figure 4A and B). This could indicate that the P43L mutation is able to limit disulfide bond scrambling during expression, resulting in a decrease in the amount of multimers.

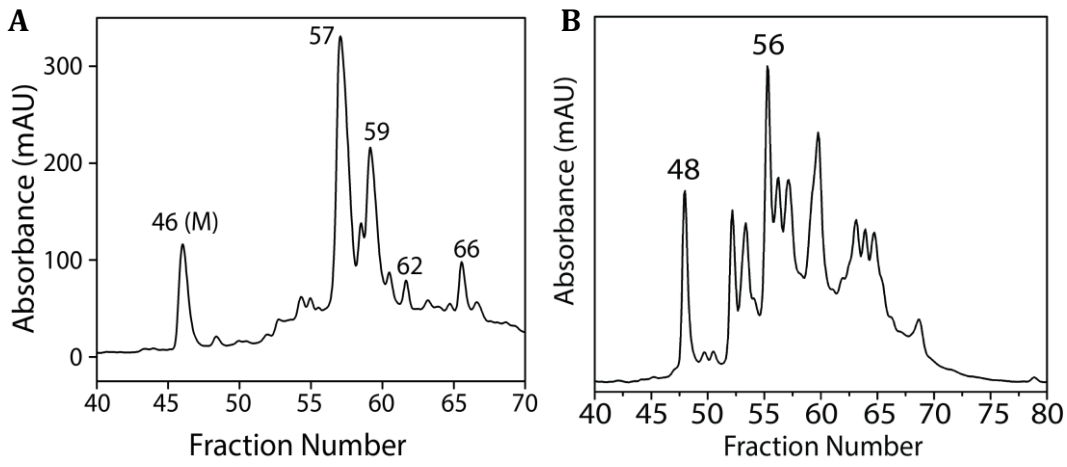

Figure 4: HPLC Profiles. A- P43LGRN3 monomer elutes in fraction 46 and forms far less multimers than does GRN-3. **B**- Native GRN-3 monomer elutes at fraction 48 and forms extensive multimers.

4.2 Characterization of the protein

4.2.1 SDS PAGE Analysis

Selected fractions from the HPLC were run on an 8-16% SDS-PAGE gel under reducing and non-reducing conditions (Figure 5). All lanes showed an intense band between 3.5 and 10 kDa corresponding to the 6.3 kDa molecular weight of monomeric P43LGRN-3. Many lanes, both reduced and non-reduced, also presented extensive banding and smearing, indicating that P43LGRN-3 forms disulfide-bonded multimers.

Lanes 1 and 2, represent the reduced and non-reduced samples of HPLC fraction 46 that differ from the other lanes in that the non-reduced lane showed a negligible amount of multimers except for a faint dimeric band, which we conclude is the intramolecularly disulfide bonded monomer.

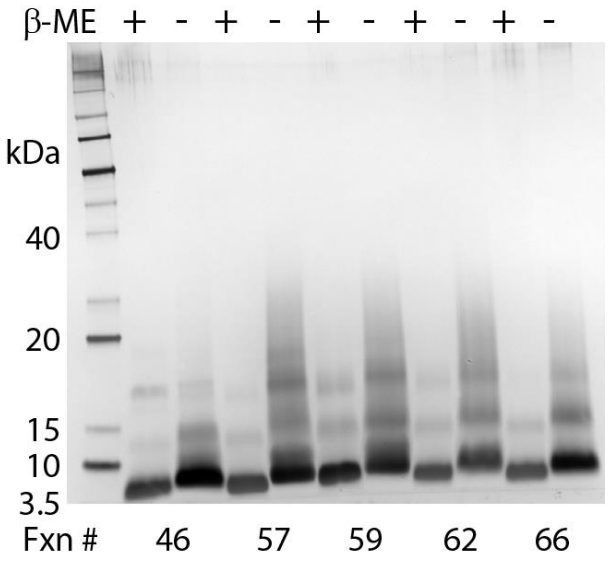

Figure 5: SDS-PAGE (8-16%) analysis of HPLC fractions. Fraction 46 shows minimal banding in both lanes.

4.2.2 MALDI-ToF Mass Spectrometry

To conclusively identify the monomeric fraction, selected fractions were analyzed using MALDI-ToF mass spectrometry. The profiles can be seen in Figure 6A-B. In the fraction 46 spectra, there was an intense peak of molecular weight 6375.29 Da corresponding to the molecular weight of monomeric P43LGRN-3. There was also a relatively small dimeric peak, corroborating the faint band seen on the SDS-PAGE gel image. When compared to spectra obtained from the analysis of other fractions, it was clear that the ratio for monomer to dimer was much higher in the multimeric fraction and

that the peaks corresponding to higher-level multimers were absent. This confirmed that fraction 46 was indeed the monomeric P43LGRN-3 fraction.

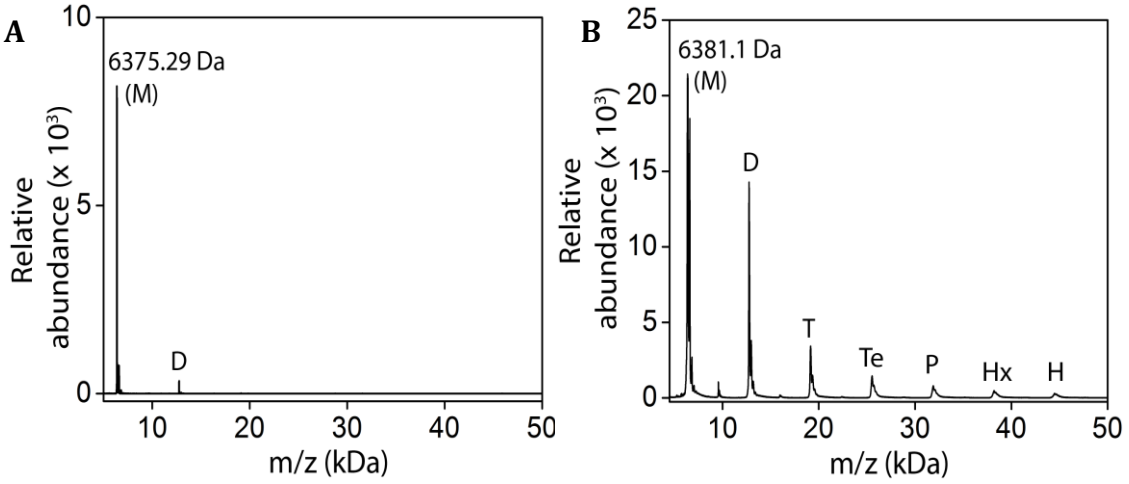

Figure 6: **MALDI-ToF spectra. A-** P43LGRN-3 fraction 46 exhibits an intense monomeric peak of molecular weight 63675.29 Da and a relatively small dimeric peak. **B-** Fraction 57 shows a much higher relative ratio of monomer to dimer as well as several other multimers.

4.2.3 Ellman's Assay

Using Ellman's Assay, the percentage of free cysteines present in the monomeric and multimeric HPLC fractions was found. The monomeric fraction showed that approximately 1% (0.8%) of the cysteines was free. This low percentage suggests that all six disulfide bonds were present and that the protein was in its completely oxidized state. The percentage of free cysteines in the multimeric fraction was zero.

4.2.4 Circular Dichroism

Monomeric P43LGRN-3 was also subjected to CD spectroscopy analysis. The spectra exhibited a minimum at ~200 nm, which is characteristic of random coil structure

(Figure 7A). This minimum could also be seen in the CD spectra of wild-type GRN-3 (Figure 7B). However, some spectral difference existed between the mutant and wild-type, namely the slight maximum that is seen at ~230 nm in the P43LGRN-3 spectra. This maximum was absent in the wild-type protein, which could suggest that the mutant form exhibited characteristics of a poly proline type II helix (PPII). Random coil structures and PPII helices share similar arrangement of amide dipoles and, as such, both are commonly observed conformations for IDPs.

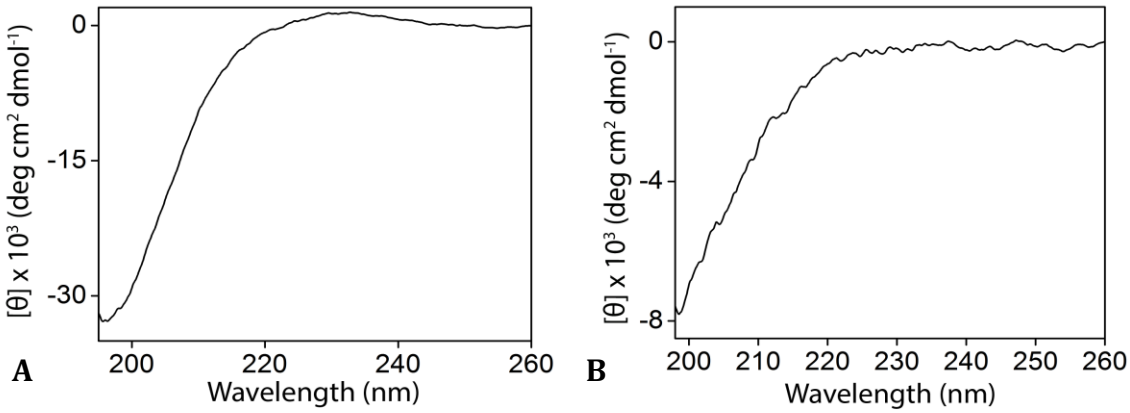

Figure 7: CD Spectra. A- P43LGRN-3 exhibits a random coil structure with characteristic minima at approximately 200 nm. **B-** Wild-type GRN-3 also exhibits random coil structure. No appreciable differenced exist between the profiles.

4.2.5 Intrinsic Tryptophan Fluorescence

To investigate whether P43LGRN-3 was forming non-covalent dimers as seen in the non-reduced monomeric lane on the SDS-PAGE gel (refer to Figure 5), tryptophan fluorescence was monitored as a function of protein concentration. Any change in W fluorescence with dilution can be correlated to formation of dimers via non-covalent interactions such as hydrophobic interactions. Upon dilution and normalization of data, an exponential response was seen in the P43LGRN-3 sample (Figure 8). Conversely, the negative control, performed with bovine serum albumin (BSA), did not show an

exponential response, indicating that the changes in tryptophan fluorescence were unique to P43LGRN-3. These data provided indirect evidence that P43LGRN-3 does form non-covalent dimers.

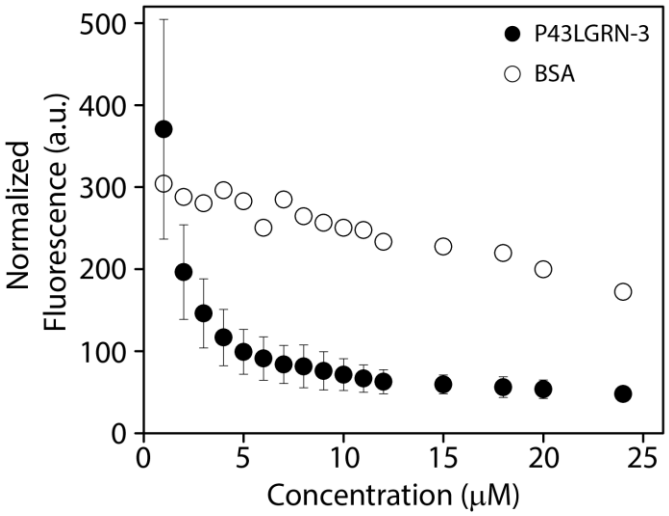

Figure 8: Tryptophan Fluorescence. An exponential response is seen with P43LGRN-3. The negative control shows no such response.

4.3 P43LGRN-3 Interactions with wt-Aβ42

4.3.1 P43LGRN-3 and wt-Aβ42 Co-incubations

Freshly purified wt-Aβ42 (20 μM) was co-incubated with 4 μM (substoichiometric) and 40 μM (superstoichiometric) concentrations of P43LGRN-3. Aggregation of Aβ was monitored using ThT fluorescence and western immunoblotting with a primary antibody specific for Aβ. Figure 9 shows the ThT data plotted over a period of 50 hours. The data shows that substoichiometric concentrations of P43LGRN-3 did not have an appreciable effect on the initial aggregation of Aβ. However, superstoichiometric incubation exhibited a drastic acceleration in aggregation within the

first 36 hours of incubation. A superstoichiometric concentration of wild-type GRN-3 was also included in the experiment. As seen in the figure, the effect of wild-type GRN-3 and P43LGRN-3 on Aβ aggregation were similar.

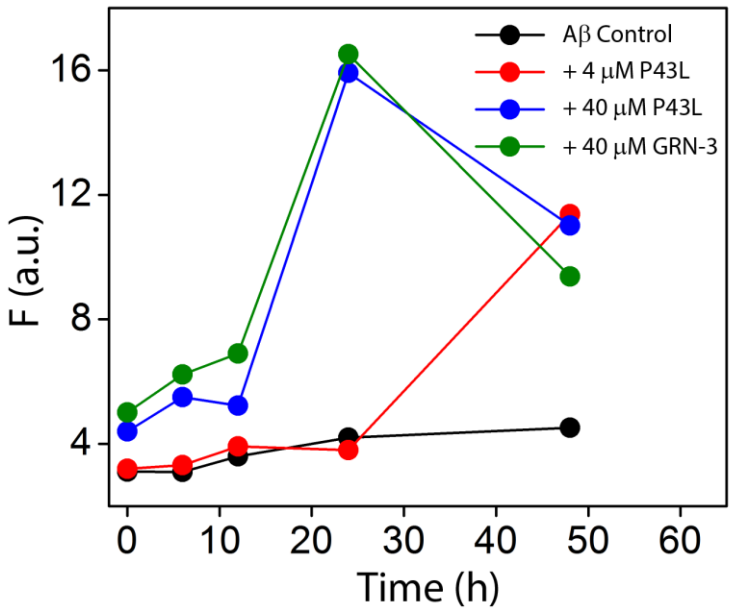

Figure 9: ThT Co-incubation Data. A drastic acceleration in aggregation of Aβ is seen with 40 μM P43LGRN-3 and wild-type GRN-3.

The co-incubation was also monitored using ThT fluorescence via western immunoblotting at the 6 and 12 hour time points (Figure 10). After 6 hours, Lane 3, which corresponds to Aβ incubated with 40 μM P43LGRN-3, showed a high molecular weight aggregate. This indicates that within 6 hours, P43LGRN-3 was causing Aβ to aggregate into fibrils. The same pattern can also be seen after 12 hours. No such

aggregate was seen in the Aβ control lane or the lane with Aβ incubated with 4 μM P43LGRN-3. The 40 μM wild-type GRN-3 incubated with Aβ, seen in lane 4, behaved similarly to 40 μM P43LGRN-3, exhibiting a high molecular weight aggregate after 6 hours.

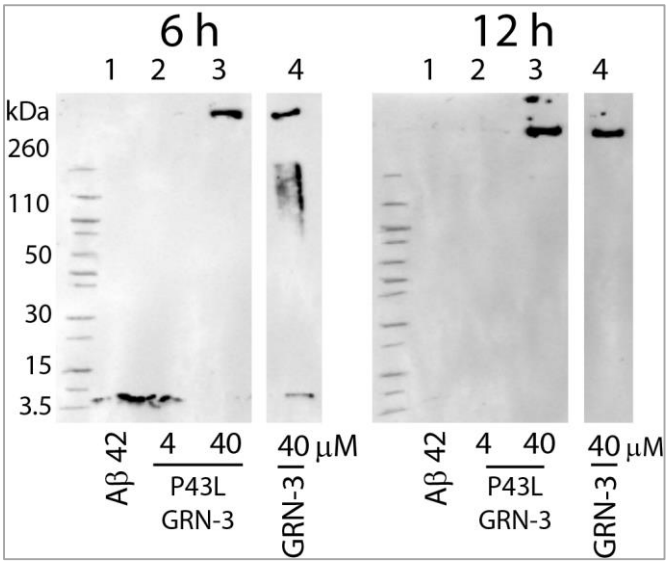

Figure 10: Western Immunoblots (6 hr and 12 hr) A high molecular weight band is seen in the 40 μM lane of P43LGRN-3 after 6 hours. The same can be seen in lane 4 (40 μM GRN-3) after 6 hours. 12 hr blot shows same activity.

Chapter 5 – Conclusions

5.1 P43LGRN3 Conclusions

Amyloid-β aggregation is known to be a primary causative agent in the onset and progression of AD, yet the molecular underpinnings of the pathology remain unclear. Emerging evidence suggests that acute neuroinflammation could trigger initial Aβ aggregation. Our hypothesis that granulins could be a key modulator of inflammation and dementia is due to their pro-inflammatory nature and roles in neurodegenerative disorders. Both wt and P43LGRN-3 have been implicated in FTD, and hence are of particular interest in our laboratory.

The primary objective of my research was to identify the effect of the P43L mutation on the structure and/or function of the protein as compared to the wt GRN-3. In this context, our findings have revealed several shared characteristics between the mutant and the wt GRN-3. Structurally, both proteins are largely disordered, with P43LGRN-3 CD spectra revealing a random coil structure with possible PPII helical content (which is also a trait of intrinsically disordered proteins (IDPs). Although similar to each other in many biophysical aspects, wt and mutant GRN-3 differ in their expression of monomeric and multimeric forms. While wt GRN-3 seems to generate more multimers, P43LGRN-3 showed markedly reduced levels of multimers by HPLC fractionation (Fig 4A-B). It is unknown whether the presence of the PPII helix is responsible for the marked decrease in the formation of multimers seen on comparison of mutant and wild-type HPLC profiles. Furthermore, the physiological implications of these findings are yet to be determined. Lastly, through tryptophan fluorescence, we indirectly determined that P43LGRN-3 forms non-covalent dimers. The significance of this finding may perhaps be found in its

structural implication for the PGRN protein. Recent studies have provided evidence suggesting that the majority of secreted and circulating PGRN exists as a homodimer, but the regions required for homodimerization to occur are not known. The functional relevance of formation of Progranulin dimers is currently unknown. From a functionality standpoint, both wild-type and mutant GRN-3 have been shown to accelerate the aggregation of Aβ into fibrils. This behavior, though not unique to the P43L mutant, supports our hypothesis that Granulins, specifically GRN-3, are capable of interacting with extracellular Aβ, facilitating its aggregation, and thereby modulating the onset of inflammation-induced AD.

Our research suggests that the P43L mutation has a minimal effect on the structure and function of the GRN-3 protein, although the mutation seems to minimize the levels of intermolecularly disulfide-bonded multimers in the protein.

5.2 Future Directions

Although no differences in structure or function between the wt and mutant P43LGRN-3 were discovered in this research, we have not yet explored the effect of the P43L mutation on the full-length Progranulin structure. It is plausible that the presence of leucine is pathogenic due to its destabilization of the Progranulin structure and that it does not alter the smaller GRN-3 structure and function. This possibility will continue to be explored as this research is continued. In addition, the propensity for native GRN-3 to form extensive multimers not seen in the P43LGRN3 purification will be investigated, as this could indicate an intrinsic difference in the behavior of the two proteins.

References

1. D. J. Selkoe, Alzheimer's disease: genes, proteins, and therapy. *Physiol Rev* 81, 741 (Apr, 2001).
2. 2013 Alzheimer's disease facts and figures. *Alzheimer's & dementia : the journal of the Alzheimer's Association* 9, 208 (2013).
3. M. Heneka, M. K. O'Banion, D. Terwel, M. Kummer, Neuroinflammatory processes in Alzheimer's disease. *J Neural Transm* 117, 919 (2010/08/01, 2010).
4. J. Zhu *et al.*, Conversion of proepithelin to epithelins: roles of SLPI and elastase in host defense and wound repair. *Cell* 111, 867 (Dec 13, 2002).
5. Johnson, V. E., Stewart, W., and Smith, D. H. (2010) Traumatic brain injury and amyloid-[beta] pathology: a link to Alzheimer's disease? *Nat Rev Neurosci* 11, 361-370
6. J. Hardy, D. J. Selkoe, The Amyloid Hypothesis of Alzheimer's Disease: Progress and Problems on the Road to Therapeutics. *Science* 297, 353 (July 19, 2002, 2002).
7. Z. Ahmed, I. Mackenzie, M. Hutton, D. Dickson, Progranulin in frontotemporal lobar degeneration and neuroinflammation. *Journal of Neuroinflammation* 4, 7 (2007).
8. C. Haass, A. Hung, D. Selkoe, Processing of beta-amyloid precursor protein in microglia and astrocytes favors an internal localization over constitutive secretion. *The Journal of Neuroscience* 11, 3783 (December 1, 1991, 1991).
9. P. Sorrentino, A. Iuliano, A. Polverino, F. Jacini, G. Sorrentino, The dark sides of amyloid in Alzheimer's disease pathogenesis. *FEBS Letters* 588, 641 (2014).

10. K. Herrup, Reimagining Alzheimer's Disease—An Age-Based Hypothesis. *The Journal of Neuroscience* 30, 16755 (December 15, 2010, 2010).
11. P. Ghosh, A. Kumar, B. Datta, V. Rangachari, Dynamics of protofibril elongation and association involved in Abeta42 peptide aggregation in Alzheimer's disease. *BMC Bioinformatics* 11, S24 (2010).
12. K. Ono, M. Yamada, Low-n oligomers as therapeutic targets of Alzheimer's disease. *Journal of Neurochemistry* 117, 19 (2011).
13. R. N. Kalaria, Microglia and Alzheimer's disease. *Current Opinion in Hematology* 6, 15 (1999).
14. P. Eikelenboom *et al.*, The significance of neuroinflammation in understanding Alzheimer's disease. *J Neural Transm* 113, 1685 (2006/11/01, 2006).
15. A. Bateman, H. P. Bennett, Granulins: the structure and function of an emerging family of growth factors. *J Endocrinol* 158, 145 (Aug, 1998).
16. G. Serrero, Autocrine growth factor revisited: PC-cell-derived growth factor (progranulin), a critical player in breast cancer tumorigenesis. *Biochemical and Biophysical Research*
17. L. M. Liau *et al.*, Identification of a Human Glioma-associated Growth Factor Gene, granulin, Using Differential Immuno-absorption. *Cancer Research* 60, 1353 (March 1, 2000, 2000).
18. N. Matsumura *et al.*, Oncogenic Property of Acrogranin in Human Uterine Leiomyosarcoma: Direct Evidence of Genetic Contribution in In vivo Tumorigenesis. *Clinical Cancer Research* 12, 1402 (March 1, 2006, 2006).

19. J. Xu *et al.*, Extracellular progranulin protects cortical neurons from toxic insults by activating survival signaling. *Neurobiology of Aging* 32, 2326.e5 (2011).
20. X. Gao *et al.*, Progranulin promotes neurite outgrowth and neuronal differentiation by regulating GSK-3β. *Protein Cell* 1, 552 (2010/06/01, 2010).
21. Baker, M., Mackenzie, I. R., Pickering-Brown, S. M., Gass, J., Rademakers, R., Lindholm, C., Snowden, J., Adamson, J., Sadovnick, A. D., Rollinson, S., Cannon, A., Dwosh, E., Neary, D., Melquist, S., Richardson, A., Dickson, D., Berger, Z., Eriksen, J., Robinson, T., Zehr, C., Dickey, C. A., Crook, R., McGowan, E., Mann, D., Boeve, B., Feldman, H., and Hutton, M. (2006) Mutations in progranulin cause tau-negative frontotemporal dementia linked to chromosome 17. *Nature* 442, 916-919
22. G. Rabinovici, B. Miller, Frontotemporal lobar degeneration. *CNS Drugs* 24, 375 (2010/05/01, 2010).
23. M. Engelhart *et al.*, Inflammatory proteins in plasma and the risk of dementia: the rotterdam study. *Arch Neurol* 61, 668 (2004).
24. S. Weggen, M. Rogers, J. Eriksen, NSAIDs: small molecules for prevention of Alzheimer's disease or precursors for future drug development? *Trends in Pharmacological Sciences* 28, 536 (2007).
25. S. Weggen, *et al.* A subset of NSAIDs lower amyloidogenic Aβ42 independently of cyclooxygenase activity. Nature, 414 (2001), pp. 212–216
26. J.L. Eriksen, *et al.* NSAIDs and enantiomers of flurbiprofen target γ-secretase and lower Aβ42 *in vivo*. J. Clin. Invest., 112 (2003), pp. 440–449

27. Roberts GW, et al. Beta amyloid protein deposition in the brain after severe head injury: implications for the pathogenesis of Alzheimer's disease. J Neurol Neurosurg Psychiatry. 1994;57:419–425.
28. Rohrer, J. D.; Ridgway, G. R.; Modat, M.; Ourselin, S.; Mead, S.; Fox, N. C.; Rossor, M. N.; Warren, J. D. Distinct profiles of brain atrophy in frontotemporal lobar degeneration caused by progranulin and tau mutations. NeuroImage, 53 (3), (2010) pp.1070–1076.
29. Shankaran, S. S.; Capell, A.; Hruscha, A. T.; Fellerer, K.; Neumann, M.; Schmid, B.; Haass, C. Missense Mutations in the Progranulin Gene Linked to Frontotemporal Lobar Degeneration with Ubiquitin- immunoreactive Inclusions Reduce Progranulin Production and Secretion. Journal of Biological Chemistry 2007, 283 (3), 1744–1753.
30. Zee, J. V. D.; Ber, I. L.; Maurer-Stroh, S.; Engelborghs, S.; Gijselinck, I.; Camuzat, A.; Brouwers, N.; Vandenberghe, R.; Sleegers, K.; Hannequin, D.; Dermaut, B.; Schymkowitz, J.; Campion, D.; Santens, P.; Martin, J.-J.; Lacomblez, L.; Pooter, T. D.; Peeters, K.; Mattheijssens, M.; Vercelletto, M.; Broeck, M. V. D.; Cruts, M.; Deyn, P. P. D.; Rousseau, F.; Brice, A.; Broeckhoven, C. V. Mutations other than Null Mutations Producing a Pathogenic Loss of Progranulin in Frontotemporal Dementia. Human Mutation 2007, 28 (4), 416–416.